CERN-PH-EP/2004-048

August 26, 2004

Measurement of K^0_{e3} form factors

NA48 Collaboration

A. Lai, D. Marras

Dipartimento di Fisica dell'Università e Sezione dell'INFN di Cagliari, I-09100 Cagliari, Italy

A. Bevan, R.S. Dosanjh, T.J. Gershon, B. Hay, G.E. Kalmus, C. Lazzeroni, D.J. Munday, E. Olaiya [2], M.A. Parker, T.O. White, S.A. Wotton

Cavendish Laboratory, University of Cambridge, Cambridge, CB3 0HE, U.K. [1]

G. Barr, G. Bocquet, A. Ceccucci, T. Cuhadar-Dönszelmann, D. Cundy [3], G. D'Agostini, N. Doble [4], V. Falaleev, L. Gatignon, A. Gonidec, B. Gorini, G. Govi, P. Grafström, W. Kubischta, A. Lacourt, A. Norton, S. Palestini, B. Panzer-Steindel, H. Taureg, M. Velasco [5], H. Wahl [6]

CERN, CH-1211 Genève 23, Switzerland

C. Cheshkov [7], P. Hristov [7], V. Kekelidze, L. Litov [7], D. Madigojine, N. Molokanova, Yu. Potrebenikov, S. Stoynev, A. Zinchenko

Joint Institute for Nuclear Research, Dubna, 141980, Russian Federation

I. Knowles, V. Martin [5], R. Sacco [9], A. Walker

Department of Physics and Astronomy, University of Edinburgh, JCMB King's Buildings, Mayfield Road, Edinburgh, EH9 3JZ, U.K.

M. Contalbrigo, P. Dalpiaz, J. Duclos, P.L. Frabetti [10], A. Gianoli, M. Martini, F. Petrucci, M. Savrié

Dipartimento di Fisica dell'Università e Sezione dell'INFN di Ferrara, I-44100 Ferrara, Italy

Submitted to Physics Letters B

A. Bizzeti [11], M. Calvetti, G. Collazuol [4], G. Graziani [12],
E. Iacopini, M. Lenti, F. Martelli [13], M. Veltri [13]

Dipartimento di Fisica dell'Università e Sezione dell'INFN di Firenze, I-50125 Firenze, Italy

H.G. Becker, K. Eppard, M. Eppard [7], H. Fox [5], A. Kalter,
K. Kleinknecht, U. Koch, L. Köpke, P. Lopes da Silva,
P. Marouelli, I. Pellmann [15], A. Peters [7], B. Renk, S.A. Schmidt,
V. Schönharting, Y. Schué, R. Wanke, A. Winhart,
M. Wittgen [16]

Institut für Physik, Universität Mainz, D-55099 Mainz, Germany [14]

J.C. Chollet, L. Fayard, L. Iconomidou-Fayard, J. Ocariz,
G. Unal, I. Wingerter-Seez

Laboratoire de l'Accélérateur Linéaire, IN2P3-CNRS,Université de Paris-Sud, 91898 Orsay, France [17]

G. Anzivino, P. Cenci, E. Imbergamo, P. Lubrano,
A. Mestvirishvili, A. Nappi, M. Pepe, M. Piccini

Dipartimento di Fisica dell'Università e Sezione dell'INFN di Perugia, I-06100 Perugia, Italy

L. Bertanza, R. Carosi, R. Casali, C. Cerri, M. Cirilli [7],
F. Costantini, R. Fantechi, S. Giudici, I. Mannelli,
G. Pierazzini, M. Sozzi

Dipartimento di Fisica, Scuola Normale Superiore e Sezione dell'INFN di Pisa, I-56100 Pisa, Italy

J.B. Cheze, J. Cogan, M. De Beer, P. Debu, A. Formica,
R. Granier de Cassagnac, E. Mazzucato, B. Peyaud, R. Turlay,
B. Vallage

DSM/DAPNIA - CEA Saclay, F-91191 Gif-sur-Yvette, France

M. Holder, A. Maier, M. Ziolkowski

Fachbereich Physik, Universität Siegen, D-57068 Siegen, Germany [18]

R. Arcidiacono, C. Biino, N. Cartiglia, F. Marchetto,
E. Menichetti, N. Pastrone

Dipartimento di Fisica Sperimentale dell'Università e Sezione dell'INFN di Torino, I-10125 Torino, Italy

J. Nassalski, E. Rondio, M. Szleper [5], W. Wislicki, S. Wronka

Soltan Institute for Nuclear Studies, Laboratory for High Energy Physics, PL-00-681 Warsaw, Poland [19]

H. Dibon, G. Fischer, M. Jeitler, M. Markytan, I. Mikulec,
G. Neuhofer, M. Pernicka, A. Taurok, L. Widhalm

Österreichische Akademie der Wissenschaften, Institut für Hochenergiephysik, A-1050 Wien, Austria [20]

---

[1] Funded by the U.K. Particle Physics and Astronomy Research Council
[2] Present address: Rutherford Appleton Laboratory, Chilton, Didcot, Oxon, OX11 0QX, U.K.
[3] Present address: Istituto di Cosmogeofisica del CNR di Torino, I-10133 Torino, Italy
[4] Present address: Dipartimento di Fisica, Scuola Normale Superiore e Sezione dell'INFN di Pisa, I-56100 Pisa, Italy
[5] Present address: Northwestern University, Department of Physics and Astronomy, Evanston, IL 60208, USA
[6] Present address: Dipartimento di Fisica dell'Università e Sezione dell'INFN di Ferrara, I-44100 Ferrara, Italy
[7] Present address: PH department, CERN, CH-1211 Genève 23, Switzerland
[8] Present address: Carnegie Mellon University, Pittsburgh, PA 15213, USA
[9] Present address: Laboratoire de l'Accélérateur Linéaire, IN2P3-CNRS,Université de Paris-Sud, 91898 Orsay, France
[10] Present address: Joint Institute for Nuclear Research, Dubna, 141980, Russian Federation
[11] Dipartimento di Fisica dell'Università di Modena e Reggio Emilia, I-41100 Modena, Italy
[12] Present address: DSM/DAPNIA - CEA Saclay, F-91191 Gif-sur-Yvette, France
[13] Istituto di Fisica dell'Università di Urbino, I-61029 Urbino, Italy
[14] Funded by the German Federal Minister for Research and Technology (BMBF) under contract 7MZ18P(4)-TP2
[15] Present address: DESY Hamburg, D-22607 Hamburg, Germany
[16] Present address: SLAC, Stanford, CA 94025, USA
[17] Funded by Institut National de Physique des Particules et de Physique Nucléaire (IN2P3), France
[18] Funded by the German Federal Minister for Research and Technology (BMBF) under contract 056SI74
[19] Supported by the KBN under contract SPUB-M/CERN/P03/DZ210/2000 and using computing resources of the Interdisciplinary Center for Mathematical and Computational Modelling of the University of Warsaw.
[20] Funded by the Federal Ministry od Science and Transportation under the contract GZ 616.360/2-IV GZ 616.363/2-VIII, and by the Austrian Science Foundation under contract P08929-PHY.

Abstract.

The semileptonic decay of the neutral K meson, $K_L^0 \to \pi^{\pm} e^{\mp} \nu$ (K_{e3}), was used to study the strangeness-changing weak interaction of hadrons. A sample of 5.6 million reconstructed events recorded by the NA48 experiment was used to measure the Dalitz plot density. Admitting all possible Lorentz-covariant couplings, the form factors for vector ($f_+(q^2)$), scalar (f_S) and tensor (f_T) interactions were measured. The linear slope of the vector form factor $\lambda_+ = 0.0284 \pm 0.0007 \pm 0.0013$ and values for the ratios $|f_S/f_+(0)| = 0.015^{+0.007}_{-0.010} \pm 0.012$ and $|f_T/f_+(0)| = 0.05^{+0.03}_{-0.04} \pm 0.03$ were obtained. The values for f_S and f_T are consistent with zero. Assuming only Vector-Axial vector couplings, $\lambda_+ = 0.0288 \pm 0.0004 \pm 0.0011$ and a good fit consistent with pure V-A couplings were obtained. Alternatively, a fit to a dipole form factor yields a pole mass of $M = 859 \pm 18$ MeV, consistent with the $K^*(892)$ mass.

1 Introduction

The study of semileptonic decays of K_L mesons gives valuable information about the strangeness-changing weak interaction and can be used as a test for possible non-vectorial components of the weak hadronic interaction and of models of low-energy strong interactions.

The most general form of the matrix element for K_{e3} decays is given by[1] :

$$M = \sqrt{1/2} G_F \sin\theta_c \overline{u_\nu}(1-\gamma_5)[m_K f_S + (1/2i)\{(P_K+P_\pi)_\lambda f_+ + (P_K-P_\pi)_\lambda f_-\}\gamma_\lambda + i(f_T/m_K)\sigma_{\lambda\tau}[P_K]_\lambda[P_\pi]_\tau]u_l, \quad (1)$$

where θ_c is the Cabibbo angle, $\overline{u_\nu}$ and u_l are the lepton spinors, P_K and P_π are the kaon and pion four-momenta respectively and m_K is the kaon mass. The determination of the scalar (f_S), vector (f_+ and f_-) and tensor (f_T) form factors is based on measurement of the Dalitz plot density which in the kaon rest frame has the following form [2]:

$$\rho(E_\pi^*, E_e^*) \sim a[f_+(q^2)]^2 + c[f_S + \frac{1}{m_K}(E_\nu^* - E_e^*) f_T]^2, \quad (2)$$

where E_i^* is the energy of the particle i in the kaon rest frame,
$f_+(q^2) = f_+(0)(1 + \lambda_+ q^2/m_\pi^2 + \lambda'_+ q^4/m_\pi^4)$,
$a = m_K(2E_e^* E_\nu^* - m_K E_\pi{}')$,
$c = m_K^2 E_\pi{}'$,
$E_\pi{}' = \frac{(m_K^2+m_\pi^2)}{2m_K} - E_\pi^*$,
$q^2 = (m_K^2 + m_\pi^2 - 2m_K E_\pi^*)$

In the expression for the vector form factor V, the f_- contribution can be neglected because it is proportional to the electron mass squared. The dependence of the f_+ form factor on the momentum transfer q^2 and its value $f_+(0)$ at $q^2 = 0$ are of theoretical interest [3], [4], [5]. The q^2 dependence is usually assumed to follow a pole-dominance formula $f_+(q^2) = f_+(0)/(1 - q^2/M^2)$, where M is the K^* meson mass, $M = 892$ MeV. This leads in a linear

approximation to $\lambda_+ = m_\pi^2/M^2 = 0.0245$ if one uses the π^+ mass for m_π. A calculation in chiral perturbation theory to order $O(p^6)$ [3] predicts a value of $\lambda_+ = 0.022$. Other calculations in chiral perturbation theory [4] and in lattice QCD [5] concentrate on the value of $f_+(0)$, which is important for the absolute rate of K_{e3} decay.

Evidence for non-zero scalar and tensor form factors in the case of $K^+ \to \pi^0 e^+ \nu$ has been reported in [6]. Recent measurements [7], [8] of the charged decay modes have not confirmed the results of [6] however, while investigations of neutral kaon decays have revealed no significant deviation from vector type interactions ([9], [10]). The study presented here improves the statistical and systematic significance of these investigations using a measurement performed with the NA48 detector in a neutral kaon beam at the CERN SPS.

2 Experimental setup

The NA48 detector was designed for a measurement of direct CP violation in the K^0 system. Here we use data from a dedicated run in September 1999 where a K_L beam was produced by 450 GeV/c protons from the CERN SPS incident on a beryllium target. The decay region is located 120 m from the K_L target after three collimators and sweeping magnets. It is contained in an evacuated tube, 90 m long, terminated by a thin ($3 \cdot 10^{-3} X_0$) kevlar window.

The detector components relevant for this measurement include the following:

The **magnetic spectrometer** is designed to measure the momentum of charged particles with high precision. The momentum resolution is given by

$$\frac{\sigma(p)}{p} = (0.48 \oplus 0.009 \cdot p)\% \tag{3}$$

where p is in GeV/c. The spectrometer consists of four drift chambers (DCH), each with 8 planes of sense wires oriented along the projections x,u,y,v, each one rotated by 45 degrees with respect to the previous one. The spatial resolution achieved per projection is 100μm and the time resolution is 0.7 ns. The volume between the chambers is filled with helium, near atmospheric pressure. The spectrometer magnet is a dipole with a field integral of 0.85 Tm and is placed after the first two chambers. The distance between the first and last chamber is 21.8 m.

The **hodoscope** is placed downstream of the last drift chamber. It consists of two planes of scintillators segmented in horizontal and vertical strips and arranged in four quadrants. The signals are used for a fast coincidence of two charged particles in the trigger. The time resolution from the hodoscope is 200 ps per track.

The **electromagnetic calorimeter** (LKr) is a quasi-homogeneous calorimeter based on liquid krypton, with tower read out. The 13248 read-out cells have cross sections of 2 x 2 cm^2. The electrodes extend from the front to the back of the detector in a small angle accordion geometry. The LKr calorimeter measures the energies of the $e^\pm$ and γ quanta by

gathering the ionization from their electromagnetic showers. The energy resolution is :

$$\frac{\sigma(E)}{E} = (\frac{3.2}{\sqrt{E}} \oplus \frac{9.0}{E} \oplus 0.42)\% \quad (4)$$

where E is in GeV, and the time resolution for showers with energy between 3 GeV and 100 GeV is 500 ps.

The **muon veto system** (MUV) consists of three planes of scintillator counters, shielded by iron walls of 80 cm thickness. It is used to reduce the $K_L \to \pi^{\pm}\mu^{\mp}\nu$ background.

A more detailed description of the NA48 setup can be found elsewhere [11].

3 Data processing and Monte Carlo simulation

3.1 Trigger and data taking

The trigger was built in two levels. In the first level trigger, the presence of at least two hits in the hodoscope was required. In the second level trigger, the drift chamber hits were used to reconstruct tracks and at least one pair of tracks was required to have a transverse separation below 5 cm within 4.5 K_S decay lengths from the end of the last collimator. A first level control trigger requiring at least one hit in the hodoscope in coincidence with at least two tracks segments in the first DCH, downscaled 20 times, was also implemented for trigger efficiency calculations.

3.2 Event selection

The data sample consisted of about 2 TB of data from 100 million triggers, with approximately equal amounts recorded with alternating spectrometer magnet polarities. The data were reconstructed and subjected to off-line filtering. The following selection criteria were applied to the reconstructed data to identify K_{e3} decays and to reject background, keeping in mind the main backgrounds to K_{e3}, which are $K_L \to \pi^{\pm}\mu^{\mp}\nu$ ($K_{\mu 3}$) and $K_L \to \pi^+\pi^-\pi^0$ ($K_{3\pi}$):

- Each event was required to contain exactly two tracks, of opposite charge, and a reconstruced vertex in the decay region. To form a vertex, the closest distance of approach between these tracks had to be less than 3 cm. The decay region was defined by requirements that the vertex had to be between 6 and 34 m from the end of the last collimator and that the transverse distance between the vertex and the beam axis had to be less than 2 cm. These cuts were passed by 35 million events.

- The time difference between the tracks was required to be less than 6 ns. To reject muons, only events with both tracks inside the detector acceptance and without in-time hits in

the MUV system were used. For the same reason only particles with a momentum larger than 10 GeV (p_{min}) were accepted. In order to allow a clear separation of pion and electron showers, we required the distance between the entry points of the two tracks at the front face of the LKr Calorimeter (D_{lkr}) to be larger than 25 cm. As a result 14 million events remained.

- For the identification of electrons and pions, we use the ratio of the measured cluster energy, E, in the LKr calorimeter associated to a track to the momentum, p, of this track as measured in the magnetic spectrometer. The ratio E/p is shown for all tracks of the 14 million events in fig.1. For the selection of K_{e3} events, we require one track to have $0.93 < E/p < 1.10$ (electron) and the other track to have $E/p < 0.90$ (pion). 11.7 million events were accepted.

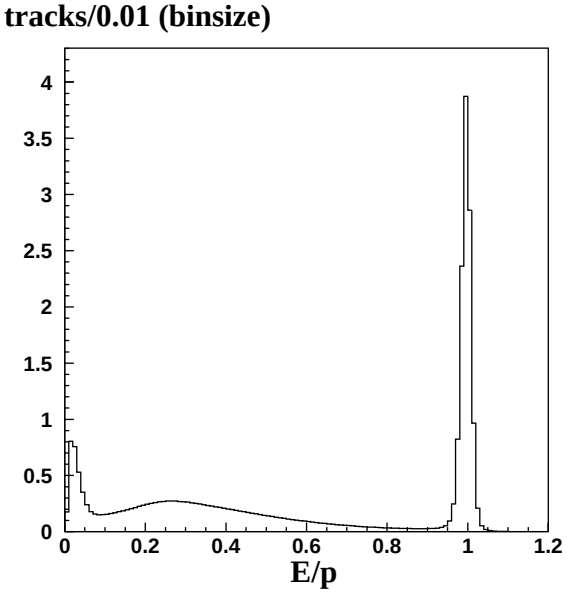

Fig. 1. Distribution of the ratio of the shower energy E reconstructed by the LKr and the momentum p reconstructed by the spectrometer.

- In order to reduce background from $K_{3\pi}$ decays, we required the quantity

$$P_0'^2 = \frac{(m_K^2 - m_{+-}^2 - m_{\pi^0}^2)^2 - 4(m_{+-}^2 m_{\pi^0}^2 + m_K^2 p_\perp^2)}{4(p_\perp^2 + m_{+-}^2)} \tag{5}$$

to be less than $-0.004(\mathrm{GeV/c})^2$. In the equation above, $p_\perp$ is the transverse momentum of the two track system (assumed to consist of two charged pions) relative to the K_L^0 flight direction and m_{+-} is the invariant mass of the charged system. The variable $P_0'^2$ peaks at zero if the charged particles are pions from the decay $K_{3\pi}$. The cut removes $(98.94 \pm 0.03)\%$ of $K_{3\pi}$ decays and $(1.03 \pm 0.02)\%$ of K_{e3} decays as estimated with the Monte Carlo simulation (Sect. 3.4). After this cut, we were left with 11.4 million K_{e3} candidate events.

The neutrino momentum in K_{e3} decays is not known and the kinematic reconstruction of the kaon momentum from the measured track momenta leads to a two-fold ambiguity in the reconstructed kaon momentum. In order to measure the kaon momentum spectrum, we selected events in which both solutions for the kaon momentum lie in the same bin of width 8 GeV. These $4 \cdot 10^5$ events we call "diagonal events".

The last selection criteria were the following two requirements: each solution for the kaon energy had to be in the energy range (60,180) GeV and the reconstructed electron and pion momenta in the center of mass of the kaon had to lie in the kinematically allowed region of the Dalitz plot for K_{e3} decays.

As a result of this selection, $5.6 \cdot 10^6$ fully reconstructed K_{e3} events were selected from the total sample.

3.3 Background

The main background to K_{e3} events arises from $K_{\mu 3}$ and $K_{3\pi}$ decays. The background from $K_{\mu 3}$ was reduced by removing events with an in-time muon signal and by the E/p requirements. The probability for a pion from $K_{\mu 3}$ to fake an electron ($E/p > 0.93$) was measured to be $5.7 \cdot 10^{-3}$. This was obtained from a sample of 75000 pion tracks from K_{e3} events where the other track had $E/p > 1.02$. The inefficiency of the MUV system for the total exposure was less than 2%. From this we estimated the number of fake K_{e3} events from $K_{\mu 3}$ to be at most 400 ± 100 events. For the suppression of background from $K_{3\pi}$ decay, we used the cut $P_0'^2 < -0.004(\mathrm{GeV/c})^2$ and the E/p requirements. The number of background events from this source is estimated to be less than 20 events.

3.4 Monte Carlo Simulation

The NA48 detector response was simulated using a GEANT-based Monte Carlo (MC) [11]. The kaon energy spectrum in the MC was taken from the kaon energy distribution reconstructed using diagonal K_{e3} events, as defined above (Sect. 3.2).

For the generation of K_{e3} MC events, the slope parameter λ_+ and the scalar and tensor form factors were set to zero. To take into account the influence of radiative corrections on the acceptance, the Photos package was used ([12]). The Dalitz plot density was then modified by the radiative corrections as calculated by Ginsberg [13]. This modification was made by randomly rejecting events according to the correct shape of the Dalitz plot. From 45 million generated MC events, 7.7 million were selected by the criteria in Sect. 3.2, corresponding to an acceptance of about 17%.

Distributions for accepted Monte Carlo events weighted with a form factor slope of $\lambda_+ = 0.029$ are shown in figs. 2, 3 and 4 together with data, for the negative magnet polarity. As an example, the distributions of charged particle momenta in the Laboratory System (figs. 2, 3) and of the neutrino energy E_ν^* in the centre-of-mass system, CMS, (fig. 4) are presented. The quantity E_ν^* is unambiguously defined. The upper part of the figures shows distributions of data, while the lower part shows the ratio of the experimental and MC spectra. Good agreement is seen for the Monte Carlo simulations with a form factor slope $\lambda_+ = 0.029$.

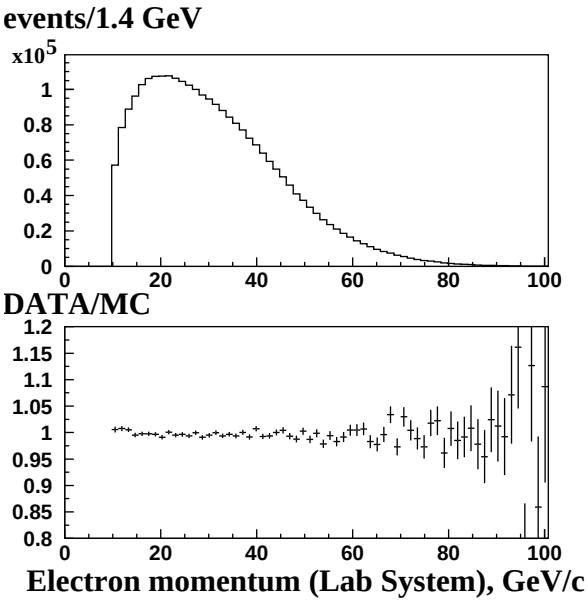

Fig. 2. Reconstructed electron momentum in the Laboratory System; data distribution and ratio data/MC

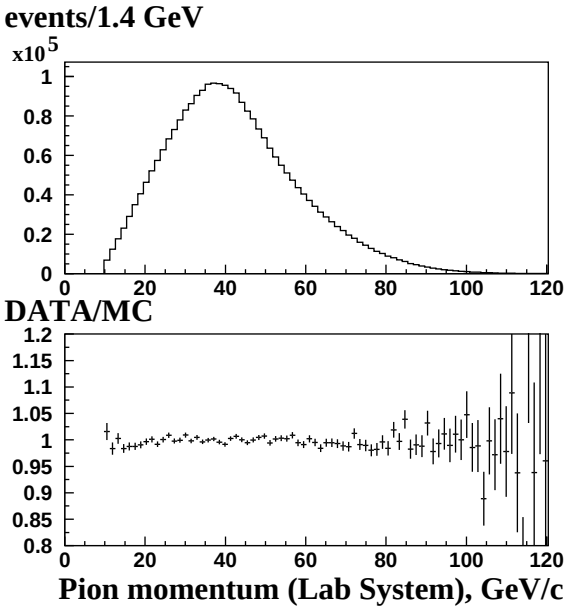

Fig. 3. Reconstructed pion momentum in the Laboratory System; data distribution and ratio data/MC

4 Data analysis

4.1 Dalitz plot analysis

For the Dalitz plot analysis, selected K_{e3} events were binned in a 19x19x19 three-dimensional array $N(E^*_\nu, q^2_1/m^2_\pi, q^2_2/m^2_\pi)$, where the indices 1 and 2 stand for the two possible solutions for the reconstructed kaon momentum and the bin sizes are 12 MeV for E^*_ν and 0.35 for the

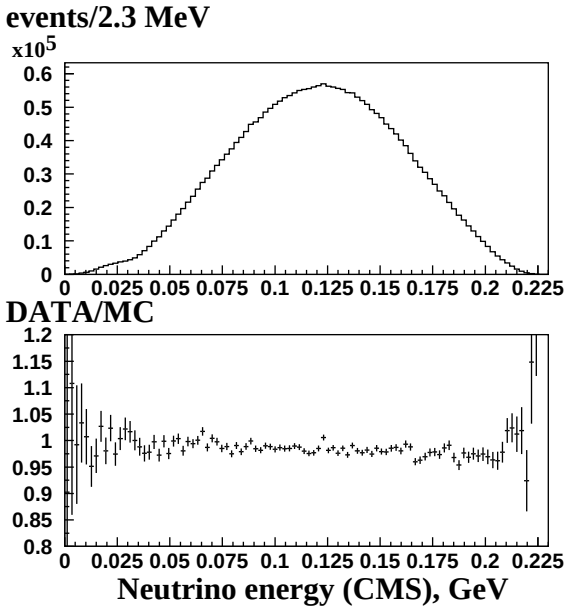

Fig. 4. Reconstructed neutrino energy E^*_ν in the Center of Mass System; data distribution and ratio data/MC

q^2/m_π^2 bins. Two-dimensional arrays $N(q_1^2/m_\pi^2, q_2^2/m_\pi^2)$ were used when pure V-A couplings were assumed.

To derive the values of the form factors we used a maximum log-likelihood method [14] based on the following likelihood function which takes into account the finite size of the MC sample:

$$\ln L = -2[\sum_{\mathrm{i}}(d_i \ln f_i - f_i) + \sum_i (a_i \ln A_i - A_i)], \tag{6}$$

Here, d_i is the number of data events in the i'th bin, f_i is the predicted number of events, a_i is the actual number of MC events and A_i is the expected number of MC events. The predicted number of events, f_i, is a function of the three form factors parameters λ_+, f_S, f_T, and is obtained by weighting the MC expectation A_i for a flat Dalitz plot with the form factors according to Eqn.2. This procedure provides a weight h_i for each bin. The MC expectation A_i for the bin i is obtained from the relation $A_i = (d_i + a_i)/(1 + h_i)$, which is valid at the maximum of the likelihood function [14], [15]. The predicted number f_i to be compared with the data d_i is then $f_i = A_i \cdot h_i$.

In order to test the goodness of fit, the variable

$$\chi^2_{gof} = [\sum_i (f_i - d_i + d_i \ln \frac{d_i}{f_i}) + \sum_i (A_i - a_i + a_i \ln \frac{a_i}{A_i})] \tag{7}$$

was used [10], [16]. The minimization of the log-likelihood function, using MINUIT [17], gives the values of the fitted form factors.

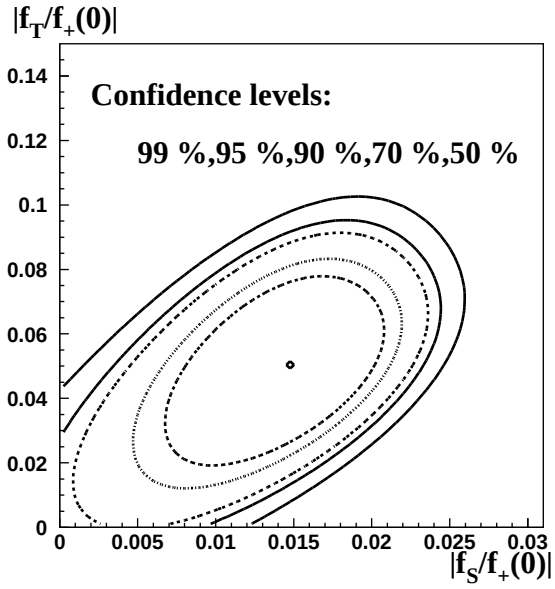

Fig. 5. Confidence level contours in the $(|f_S/f_+(0)|,|f_T/f_+(0)|)$ plane at $\lambda_+ = 0.0284$. The outermost contour corresponds to 99% C.L., the innermost to 50% C.L. Only statistical errors are considered.

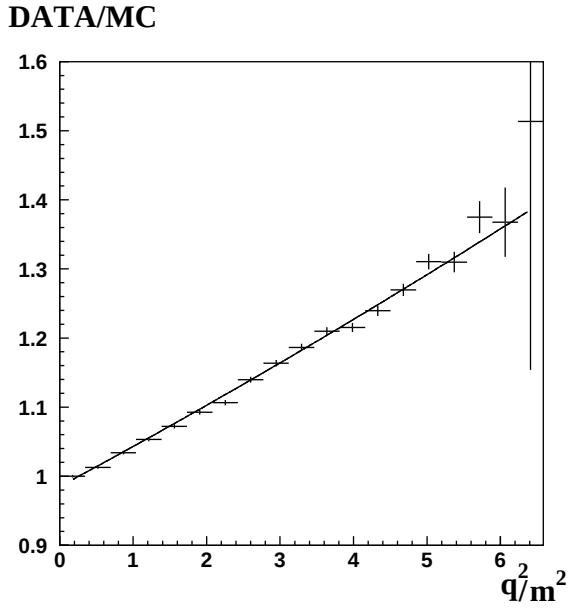

Fig. 6. Ratio of "diagonal" data and MC events (with $\lambda_+ = 0$). The vertical axis corresponds to $[f_+(q^2)/f_+(0)]^2$. The curve corresponds to $\lambda_+ = 0.0288$

4.2 Results

Linear fits.

We analysed the Dalitz plot under two hypotheses: either assuming pure V-A interaction or admitting additional scalar and tensor interactions. The results for the form factors obtained, assuming a linear q^2 dependence, are presented in Table 1. The statistical errors have

contributions from fluctuations of the data and of the MC events, as explained in sect.4.1.

Form factor	value and stat. err.	χ^2/DOF
λ_+	0.0284 ± 0.0007	3010/2915
$\lvert f_S/f_+(0)\rvert$	$0.015^{+0.007}_{-0.010}$	3010/2915
$\lvert f_T/f_+(0)\rvert$	$0.05\pm^{+0.03}_{-0.04}$	3010/2915
λ_+	0.0288 ± 0.0004	394/302
λ_+	0.0280 ± 0.0019	386/301
λ'_+	0.0002 ± 0.0004	386/301

Table 1
Results from the fits: 3-form factors case and 1-form factor case (last rows)

The confidence level contours in the ($|f_S/f_+(0)|$,$|f_T/f_+(0)|$) plane for $\lambda_+ = 0.0284$ are plotted in fig 5. The results are consistent with both f_S and f_T being zero at 10% C.L. taking only statistical errors into account.

To visualize the main feature of the two-dimensional fit we display in fig. 6 the ratio of "diagonal" data and MC events (with $\lambda_+ = 0$). "Diagonal" here means events for which both solutions for q^2 lie in one q^2/m_π^2-bin or they lie in neighbouring bins. The quantity plotted corresponds to the square of the q^2 variation of the vector form factor, $[f_+(q^2)/f_+(0)]^2 = [1 + \lambda_+ q^2/m_\pi^2]^2$. The data are seen to be consistent with a linear increase of $f_+(q^2)$ with increasing q^2.

Our investigation of possible systematic errors showed that the biggest uncertainty for λ_+ comes from the uncertainty in the kaon momentum spectrum. In order to determine the influence of this factor, the kaon momentum spectra derived from reconstructed $K \to \pi^+\pi^-$ and $K \to \pi^+\pi^-\pi^0$ decays were implemented in the MC. The differences in the fitted form factor values using either of these spectra compared to the spectrum from diagonal K_{e3} events was taken as a systematic error. This error amounts to 0.0007, and is 7 times larger than claimed in ref.[18]. We studied also the systematic errors induced by the various K_{e3} selection cuts, by the momentum and energy calibrations, Dalitz plot distributions bin width, inefficiency of the muon veto system and the trigger, possible detector asymmetries and influence of accidental particles.

The systematic uncertainties connected with our knowledge of the detector acceptance were evaluated by variations of the selection cuts in between values which changed the number of accepted events by up to 20%. The largest fluctuations in the form factor values were taken as systematic errors.

Possible shifts in the measurement of p and E were investigated by comparing the value of the reconstructed kaon mass from $K_{3\pi}$ and $K_{2\pi}$ decays with the world average for the kaon mass and by comparing the central value of the E/p distribution of electrons with unity. These led to a rescaling of p and E by $1 \cdot 10^{-3}$ and $4 \cdot 10^{-3}$ respectively. The influence on the form factor values was studied by scaling systematically p and E by the quoted amounts.

Source	$\triangle\lambda_+$	$\triangle\lvert\frac{f_S}{f_+(0)}\rvert$	$\triangle\lvert\frac{f_T}{f_+(0)}\rvert$	$\triangle\lambda_+$ only
K_L spectrum	± 0.00080	± 0.001	± 0.005	± 0.00070
Geom. accept.	± 0.00050	± 0.007	± 0.015	± 0.00040
p_{min}	± 0.00025	± 0.004	± 0.010	± 0.00015
D_{lkr}	± 0.00045	± 0.004	± 0.005	± 0.00025
E/p	± 0.00035	± 0.002	± 0.010	± 0.00035
$P_0'^2$	± 0.00020	± 0.003	± 0.005	± 0.00010
E,p scaling	± 0.00020	± 0.001	± 0.005	± 0.00020
MUV ineff.	± 0.00020	± 0.002	± 0.005	± 0.00020
Trigger ineff.	± 0.00015	± 0.002	± 0.005	± 0.00025
accidentals	± 0.00030	± 0.001	± 0.005	± 0.00025
bin width	± 0.00040	± 0.005	± 0.010	± 0.00010
TOTAL	± 0.0013	± 0.012	± 0.03	± 0.0011

Table 2
Systematic uncertainties: 3-form factors case and 1-form factor case (right column)

The inefficiency of the MUV during this run was measured to be below 2 %. In order to investigate the influence of the MUV inefficiency we introduced an extra inefficiency of 2 % in the experimental data and compared the results. The difference was taken as a systematic error.

The trigger inefficiency was evaluated by using the control trigger and was found to be $(1.9 \pm 0.1)\%$. The influence of this source of systematic uncertainty on the results was estimated as follows. The results obtained with the main trigger data for which the control trigger was set as well were compared to the results obtained with the control trigger data which are strongly correlated. The differences are due to the 2% events escaping the main trigger, and indicate the uncertainty due to this inefficiency.

To estimate the possible influence of accidental particles we used the Overlay MC technique, applied earlier in the ϵ'/ϵ analysis [11], in which randomly recorded experimental signals with rate proportional to the beam intensity were mixed with each MC event. The uncertainty due to this effect was estimated by comparing results obtained with the standard MC with results obtained with the Overlay MC.

We also varied the number of bins (from 10 to 25 in each axis) in the distributions $N(E_\nu, q_1^2, q_2^2)$ and $N(q_1^2, q_2^2)$. The change in the values of the fit parameters was considered as a systematic error.

The individual systematic uncertainties, and the total systematic error obtained by combining the individual errors in quadrature, are summarized in table 2.

As a cross check, correlations between magnetic field polarities, positive and negative tracks, particles and anti-particles, geometrical positions of the tracks were explored. We did not

find significant changes in results coming from these sources. The effect of the uncertainties of the radiative corrections [13] was found to have a negligible effect on the results.

Quadratic and dipole fits.

As an alternative to these linear slope fits, we also investigated two other forms of the q^2 dependence: a quadratic form, admitting a finite λ'_+ as a free parameter, and a pole-dominance form factor of the form given in Sect.1, with the mass of the vector meson pole mass M_V as the only free parameter. The quadratic fit gave the values of the two slope coefficients, $\lambda_+ = (28.0 \pm 1.9 \pm 1.5) \cdot 10^{-3}$ and $\lambda'_+ = (0.2 \pm 0.4 \pm 0.2) \cdot 10^{-3}$, consistent with no quadratic term but also consistent with a dipole form factor where the quadratic term of the Taylor expansion corresponds to $\lambda'_+ = \lambda_+^2 = 0.7 \cdot 10^{-3}$. The dipole fit with the vector meson mass as free parameter gave $M_V = 859 \pm 18$ MeV, fully consistent with the mass of the $K^*(892)$ meson.

5 Conclusions

Using 5.6 million K_{e3} events recorded by the NA48 detector, we tested the validity of the V-A weak interaction and measured the q^2 dependence of the vector form factor with high precision. Admitting scalar and tensor couplings in addition to V-A couplings , we obtain the following form factor values :

$$|\tfrac{f_S}{f_+(0)}| = 0.015^{+0.007}_{-0.010} \pm 0.012$$

$$|\tfrac{f_T}{f_+(0)}| = 0.05^{+0.03}_{-0.04} \pm 0.03$$

and the linear slope in the vector form factor $\lambda_+ = (28.4 \pm 0.7 \pm 1.3) \cdot 10^{-3}$. The 90% C.L. upper limits on the scalar and tensor form factors are $|\tfrac{f_S}{f_+(0)}| < 0.041$ and $|\tfrac{f_T}{f_+(0)}| < 0.12$. We therefore see no evidence for scalar or tensor couplings, not supporting the results of ref. [6].

Assuming only V-A currents and a linear q^2 dependence the λ_+ value is $\lambda_+ = (28.8 \pm 0.4 \pm 1.1) \cdot 10^{-3}$. If in addition we admit quadratic terms , the results are $\lambda_+ = (28.0 \pm 1.9 \pm 1.5) \cdot 10^{-3}$ and $\lambda'_+ = (0.2 \pm 0.4 \pm 0.2) \cdot 10^{-3}$. We therefore find no evidence for a quadratic term λ'_+ different from zero. However, the size of a quadratic term is consistent with a Taylor expansion of a pole-dominance form factor. Such a dipole form factor is in good agreement with the data, with a pole mass of 859 ± 18 MeV.

Fig. 7 shows the linear slope.

Our results agree well with the V-A coupling of the weak interaction and with a pole form of the form factor, in agreement with the linear approximations tested in former experiments [9], [18], [19], [20], [21], [22], [23]. Our result for the quadratic term in the vector form factor is at variance with the result of ref. [18] though it agrees with the pole model form factor.

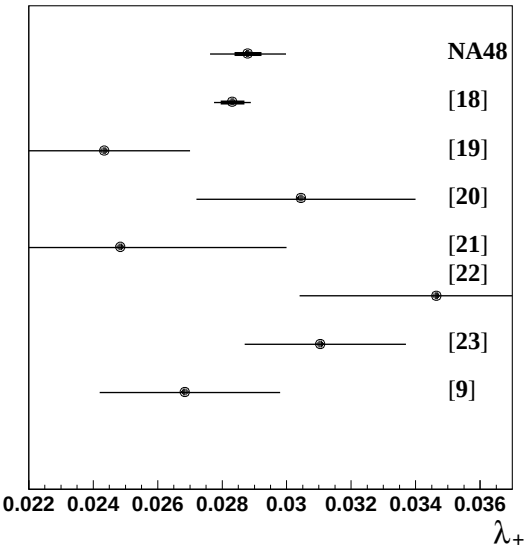

Fig. 7. Experimental results for the slope λ_+ of the vector form factor. The bold error bars are the statistical errors, while the thin line indicates the total uncertainty including the systematic error.

References

[1] H.Braun et al., Nucl. Phys. B89 (1975)210

[2] M.V. Chizhov, Phys. Lett. B381 (1996)359

[3] P.Post and K.Schilcher, Eur. Phys. J. C25 (2002)427

[4] V.Cirigliano et al., Eur. Phys. J. C35 (2004)53

[5] D.Becirevic et al., hep-ph/0403217

[6] S.A.Akimenko et al., Phys. Lett. B259 (1991)225

[7] I.Ajinenko et al., Phys. At. Nucl. 65 (2002)2064, Yad. Fiz. 65 (2002)2125

[8] A.S.Levchenko et al., Phys. At. Nucl. 65 (2002)2232, Yad. Fiz. 65 (2002)2294

[9] R.Blumenthal et al., Phys. Rev. Lett. 34 (1975)164

[10] K. Hagiwara et al., Phys. Rev. D 66 (2002)010001

[11] A.Lai et al., The NA48 Collaboration, Eur. Phys. J. C22 (2001)231

[12] E.Barberio and Z.Was, CERN-TH.7033/93

[13] E.S.Ginsberg, Phys. Rev. 171 (1968)1675, Errata: Phys. Rev. 174 (1968)2169, Phys. Rev. 187 (1969)2280

[14] R.Barlow and C.Beeston, Comp. Phys. Comm. (1993)77

[15] S. Stoynev, JINR-E1-2003-103 (2003)

[16] S.Baker and R.Cousins, Nucl. Instr. Meth. 221 (1984)437

[17] CN/ASD Group. MINUIT - Users guide (Version 94.1), nProgram Library D506. CERN, 1994.

[18] KTeV Collaboration (T. Alexopoulos et al.), hep-ex/0406003

[19] A.Apostolakis et al., Phys. Lett. B473 (2000)186

[20] R.K.Birulev et al., Nucl. Phys. B182 (1981)1

[21] A.Engler et al., Phys. Rev. D18 (1978)623

[22] D.G.Hill et al., Phys. Lett. 73B (1978)483

[23] S.Gjesdal et al., Nucl. Phys. B109 (1976)118